ORIGINAL RESEARCH ARTICLE

MRI features for predicting the pathological grade of HCC in patients undergoing liver transplantation

Aylin Altan Kus[1*] , Selim Keceoglu[2] and Ali Ozer[2]

Abstract

Background Contrast-enhanced magnetic resonance imaging (MRI) plays a crucial role in the diagnosis of hepatocellular carcinoma (HCC). This study aims to assess the performance of MRI features for evaluating hepatocellular carcinoma (HCC) aggressiveness in living liver transplantation in patients.

Material and methods This retrospective study included patients who underwent liver transplantation in our hospital between 2015 and 2020. Abdominal contrast-enhanced MRIs of these patients were reviewed, and clinical, radiological, and histopathological findings of HCCs were recorded. The prognostic features of HCCs as determined by MRI were compared with Edmondson-Steiner (E-S) grades. Liver parenchyma fibrosis based on an apparent diffusion coefficient (ADC) map was correlated with histological subclassification of cirrhosis using the Laennec staging system.

Results The study subjects included 37 men and 8 women with a mean age of 59.56 ± 7.81 (range: 25–72). The mean tumour size was 37.33 ± 22.27 mm (range: 10–118 mm), and nine tumours (23.1%) involved portal vein tumour thrombosis. There was a significant correlation between tumour grade and size ($p = 0.007$) and intratumoral fat ($p = 0.014$) even though no significant correlations between grade and mean ADC value, capsule appearance, presence of satellite lesions, smooth margin, imaging of the tumour feeding artery, and corona enhancement of HCC ($p > 0.05$) were found. There was a statistically significant correlation between mild (stage 4A) and moderate (stage 4B) fibrosis of non-tumorous liver parenchyma and ADC value ($p < 0.001$).

Conclusion Our study found that ADC values can be used to distinguish mild cirrhotic livers from moderate cirrhotic livers. Diffusion MRI might be used to diagnose the degree of liver fibrosis without histopathological analysis. According to our results, only intralesional fat and tumour size correlated with tumour grade, and as such, these parameters could be used as prognostic MRI biomarkers for HCC.

Keywords Hepatocellular carcinoma, Prognostic factors, Imaging, Magnetic resonance, Hepatic transplantation

*Correspondence:
Aylin Altan Kus
aylinaltan@gmail.com
[1] Acibadem Mehmet Ali Aydinlar University, Atakent Hospital,
Department of Radiology, Turgut Ozal Street, Istanbul 34000, Turkey
[2] Acibadem Mehmet Ali Aydinlar University, Atakent Hospital,
Department of Organ Transplantation, Turgut Ozal Street, Istanbul 34000,
Turkey

Background

Patients who were detected with hepatocellular carcinoma (HCC) at an early stage can benefit from curative treatments as the prognosis for HCC mainly depends on the disease stage. Imaging modalities that are repeatable and non-invasive can be used to diagnose HCC without a biopsy. Biopsy for the diagnosis of HCC is not routinely recommended because of the risk of tumour seeding, bleeding and sampling error. Additionally, imaging plays a critical role in the management of HCC because

imaging-based staging is essential for treatment selection, which includes surgical resection, liver transplantation or radiofrequency ablation. According to the current guidelines, a biopsy is performed for indeterminate nodules [1, 2].

Intralesional fat, smooth margins, small tumour size, presence of a fibrous capsule and high apparent diffusion coefficient (ADC) values are the favourable findings of HCC as discussed in many studies. Unfavourable findings of HCC are multifocality, bigger size, non-smooth margins, corona enhancement and low ADC values on diffusion-weighted images (DWI), with vascular invasion size and multifocality being the most important prognostic factors [3–5]. Mostly, the histological tumour grade, location and stage are the most important aspects for predicting the treatment outcomes of patients with cancer. However, prognosis assessment is complicated because of the biological heterogeneity of HCC relative to other solid tumours. If imaging findings could directly predict a prognosis, they would provide an excellent non-invasive alternative for individualized patient management [6, 7].

The goal of magnetic resonance imaging (MRI) is to assist a patient by providing them with the best care by accurately assessing disease status. In this respect, relating prognosis to imaging features may be as important as making a correct diagnosis using these techniques. Thus, the key roles of imaging include not only the screening and surveillance of HCC patients at risk but also prognosis determination. This study aimed at investigating the association between MRI findings and Edmondson-Steiner (E-S) grades of HCCs and comparing the ADC value of liver parenchyma with liver fibrosis according to the Laennec system [8].

Methods
Study population and design
This study considers a total of 85 patients who underwent liver transplantation between 2015 and 2020. Our institutional review board approved the study and waived the informed consent requirement. Data for all patients were freely accessible through an image archive and communication system and electronic clinical records. The inclusion criteria for our study are as follows, in order: adult patients aged 18 and older, cases diagnosed with HCC before live donor liver transplantation but not subjected to any procedures such as hepatic arterial infusion chemotherapy, systemic chemotherapy and transarterial chemoembolization for HCC and lesions larger than 10 mm, and the preoperative MRI was screened within 4 weeks.

Of these 85 patients, 40 patients who had undergone preoperative hepatic arterial infusion chemotherapy, systemic chemotherapy, transarterial chemoembolization,

lesions smaller than 10 mm, failure of radiological retrieval of data and cases with poor image quality due to motion artefacts during MRI were excluded from the study. The remaining 45 patients were enrolled in this study with pathologically confirmed HCC after total hepatectomy for liver transplantation. The patients and tumour characteristics are summarized in Table 1.

Image acquisition
All patients were examined with a 3.0-T MRI system (Skyra; Siemens Medical Solutions, Erlangen, Germany) in the transverse plane using a single, dedicated body-phased array coil with 18 anterior and spine array coils posterior with 32 coil channels.

Abdominal MRIs were acquired using the following sequences: T2-weighted half-Fourier-acquired single-shot turbo spin echo (Haste) coronal [repetition time (TR)/effective echo time (TE), 2000/91 ms], a matrix of 256×256, 5-mm slice thickness and a 1-mm gap. For dynamic MRI, Gd-EOB-DTPA (Gadovist, Bayer Schering; 1 mmol/kg) was injected as a rapid bolus and was immediately followed by a 30-ml saline flush through a power injector at a rate of 2 ml/s for both contrast media and saline. T1 vibe Dixon fat suppression was performed before and after (30–35 s, 65–70 s and 3 min) the injection of intravenous contrast agent with a delayed phase after ten minutes. The MRI parameters included TR/TE 4.02/1.29, a flip angle of 9°, a 195×320 matrix and a

Table 1 Patients and tumour characteristics

	Values
Mean age (years)	59.56 ± 7.81 (min: 25, max: 72)
Gender	
Men	37
Women	8
Size of tumour (mm)	37.33 ± 22.27 mm (min: 10, max: 118)
Histopathologic grade	
Grade 1	2
Grade 2	10
Grade 3	25
Grade 4	8
Preoperative AFP (ng/mL)	55.5 ± 92.94 (min: 1.08, max: 293)
Postoperative AFP (ng/mL)	3.64 ± 4.44 (min: 1, max:16.3)
Aetiology (*n*)	
Hepatitis B virus	17
Hepatitis C virus	12
Cryptogenic	10
NASH	3
Alcohol	2
Autoimmune	1

AFP alpha fetoprotein, *NASH* nonalcoholic steatohepatitis

3-mm slice thickness with a zero intersection gap. The DWI parameters were b values of 50, 400 and 800 s/mm^2; TR/TE 7400/41 ms; two signals; a matrix of 108×134; 6.5-mm slice thickness; and an acquisition time of 3.5 min. The acquired navigator-triggered T2-weighted turbo spin-echo (TSE) sequence had a TR range of 3870–4000 and TE of 99 ms, matrix of 384×202, superior and inferior spatial pre-saturation, chemical fat saturation, TR/TE 170/1.23–2.46, 6.5-mm slice thickness, 1.3-mm gap and a breath-hold, axial fat-saturated T2-weighted TSE sequence with TE of 100 ms, a matrix of 320×179, 3.5-mm slice thickness and 1.6-mm gap. The time interval between imaging and operation was less than 1 month.

Data analyses

Preoperative MRI features were retrospectively analysed on a picture archiving and communication system (PACS, Centricity, General Electric, USA). An abdominal radiologist with 10 years of experience, who was blind to the pathological data, qualitatively evaluated all MRI sequences. A total of 94 HCCs were detected and recorded. Capsule appearance, smooth margin, intralesional fat, macrovascular invasion, visualization of the feeding artery, corona enhancement, size, multifocality and mean ADC values were noted for each lesion. The ADC of each HCC was measured using an oval region of interest (ROI) on the ADC map. The largest ROI was placed on the nonnecrotic/solid portion of the tumour where the previously assessed vascularity was determined by dynamic imaging or by referring to DW T1 and T2 sequences.

Histological grading was performed by a senior pathologist with 20 years of experience in liver pathology according to the E-S criteria, which is the most commonly adopted grading system for HCC [2]. All lesions were divided into E-S grade groups (grade 1 = 2 lesions, grade 2 = 10 lesions, grade 3 = 25 lesions, and grade 4 = 8 lesions). Cirrhotic severity was rated according to the Laennec staging system as follows: no cirrhosis (combination of F0–F3), mild cirrhosis (F4A, marked septation with rounded contours), moderate cirrhosis (F4B, at least two broad septa) or severe cirrhosis (F4C, at least one very broad septum or many minute nodules). The degree of liver fibrosis, histopathologic tumour features, E-S grade and microvascular invasion were recorded.

Statistical analyses

All statistical analyses were performed using the R version 2.15.3 software (R Foundation for Statistical Computing, R core team 2013), and $p < 0.05$ was considered significant. The numerical variables were expressed as mean and standard deviation if they were distributed normally and median and minimum–maximum values if they were not. The causes of liver fibrosis, preoperative and postoperative AFP values, age, gender and tumour recurrence were noted.

Capsule presence, tumour size, corona enhancement, smooth margin presence, tumour feeding artery, intralesional fat, mean tumour ADC value and the liver parenchyma, macrovascular invasion and satellite nodules were recorded by a radiologist blinded to the pathology report.

According to E-S, grade 1 and 2 lesions were included in the low-grade group and grade 3 and 4 lesions were included in the high-grade group. The differences between the two groups were evaluated with a Mann-Whiney U test if they were not distributed normally. Pearson's chi-squared and Fisher's exact tests were used to investigate histopathological grade and size and the mean ADC value of HCC on DWI, smooth margin, visualization of the feeding artery, intratumoral fat appearance, corona enhancement, macro-invasion and capsule appearance were noted. The degree of liver parenchyma fibrosis was also compared based on Laennec staging with histopathological confirmation with the mean ADC value of liver parenchyma on DWI.

Results

Of the included patients, 37 (85.3%) were men and 8 were women with a median age of 59.56 ± 7.81 years (range: 25–72). The mean tumour size was 37.33 ± 22.27 mm (range: 10–118 mm), and nine tumours (23.1%) involved portal vein tumour thrombosis.

Underlying conditions included 17 patients with viral hepatitis B, 12 patients with viral hepatitis C, 2 with viral hepatitis D, 5 with the cryptogenic disease, 4 with NASH, 4 with alcoholic cirrhosis and 1 with autoimmune hepatitis. Whole liver specimens revealed that 53.3% of patients had one tumour while 28.8% had two tumours and 17.7% had ≥ 3 tumours.

The mean preoperative AFP level was found to be 55.5 ± 92.94 ng/ml (range: 1.08–293), and the mean postoperative AFP level was 3.64 ± 4.44 ng/ml (range: 1–16.3).

The mean tumour size was 37.33 ± 22.27 mm (range: 10–118). The mean ADC value of HCCs was $1040.33 \pm 210.41 \times 10^{-3}$ (range: 616–1450×10^{-3}). The degree of liver parenchyma fibrosis was mild in 25 patients and moderate in 20 patients. A recurrence of HCC happened in three patients after 6, 13 and 15 months of transplantation.

The capsule was histologically evident in 16 patients. Out of the 19 patients who were reported to have the appearance of a capsule on MRI, three cases were that of pseudocapsules, which accounted for false-positive MRI results. Intralesional fat was described in 11 patients,

Altan Kus *et al. Egyptian Liver Journal*   *(2023) 13:52*

Page 4 of 7

corona enhancement in 9 and the feeding artery of the tumour was visualized in 28 cases on MRI after contrast administration. Satellite nodules were reported in MRI reports for 21 patients but were only found in 24 patients by postoperative gross examination.

There was a significant correlation between tumour grade and tumour size ($p = 0.007$) and intratumoral fat ($p = 0.014$). However, there was no significant correlation between the grade and the mean ADC value, capsule appearance, satellite lesion, smooth margin, feeding artery or corona enhancement of HCC ($p > 0.05$). The MRI characteristics of HCC are summarized in Table 2.

The number of patients with liver specimens at fibrosis stage F4A was 28, and at F4B, it was 17. Our study demonstrated a significant statistical correlation between mild (F4A) and moderate (F4B) fibrosis and ADC values [$p < 0.001$ (Table 3)]. The ADC values of mild (4A) parenchyma fibrosis ranged from 1200 to 1400×10^{-3} s/mm² while for moderate (4B) fibrosis, it ranged from 962.5 to 1150×10^{-3} s/mm².

Discussion

The most preferred guidelines for diagnosis and management of HCC are the European Association for the Study of the Liver (EASL) and the American Association for the Study of Liver Disease (AASLD). Besides, AASLD reported another guideline for the non-invasive diagnosis of HCC referred to as Liver Imaging Reporting and Data System (Li-RADS) [4]. About these guidelines, the present study addressed the efficacy of MRI for the prognosis of HCC associated with predicting differentiation.

One of the findings of the present study indicated that the presence of intratumoral fat is related to the tumour grade. Although there are studies which reported that the benign regenerative nodules may contain intratumoral fat [9, 10], the fat-containing tumours are usually considered HCC in the literature [11].

Table 3 Liver parenchyma fibrosis degree and ADC value according to parenchyma fibrosis degree

	Parenchyma ADC (mm²/s), median (Q1, Q3)	*p*
Parenchyma fibrosis degree		< 0.001
Mild	1340×10^{-6} (1200, 1408)	
Moderate	1065×10^{-6} (962.5, 1150)	

ADC apparent diffusion coefficient

Moreover, the fatty change in HCC is assumed to be a sign of well-differentiation in most of the studies [4, 11]. When a dysplastic nodule evolves to HCC, transient hypoxia occurs that results in fatty changes during hepatocarcinogenesis. Our results related to intratumoral fat presence were similar to the literature.

Tumour size is another important feature of HCC affecting the histological grade. Small or the so-called early tumours are mostly related to well-differentiated HCCs [4, 11]. However, numerous studies have suggested that tumour size alone is not enough to predict this differentiation [11–13]. Our findings showed that tumour size is significantly associated with the grade of the tumour. The mean tumour size was found to be 37.33 mm in our study, and the rate of microvascular invasion (MIV) was 44.4%. As widely known, the tumour size is also related to the increased risk of MIV [14, 15]. Considering this relationship may explain our results.

Many studies have demonstrated that encapsulated HCCs have a better prognosis than nonencapsulated HCCs because of a lower incidence of direct liver invasion, fewer tumour microsatellites and less vascular invasion [6, 7]. However, our results are in contrast with these studies. We could not find a significant correlation between tumour capsule and tumour grade, which may be because the capsule appearance on imaging does not

Table 2 Features of HCC lesions on MRI according to groups

	Low-grade group (E-S 1 and E-S 2), median (Q1, Q3)	High-grade group (E-S 3 and E-S 4), median (Q1, Q3)	*p*
Size of HCC (mm)	20 (11.5, 33.5)	38 (28, 50)	0.007
ADC value of HCC (mm²/s)	996×10^{-6} (940.5, 1302.5)	984×10^{-6} (890, 1190)	0.534
	***n* (%)**	***n* (%)**	
Smooth margin	9 (75)	15 (46.9)	0.095
Capsule appearance	8 (66.7)	12 (36.4)	0.070
Intralesional fat	4 (33.3)	1 (3.0)	0.014
Multifocality	5 (41.7)	11 (34.4)	0.732
Feeding artery	3 (25)	14 (42.4)	0.488
Corona enhancement	4 (33.3)	19 (57.6)	0.150

HCC hepatocellular carcinoma, *ADC* apparent diffusion coefficient

Altan Kus *et al. Egyptian Liver Journal* (2023) 13:52

Page 5 of 7

always represent a true tumour capsule and may instead represent a pseudocapsule. We reported 19 patients with capsule appearance; however, only 16 were proven by histological analysis. Ishigami et al. [16] reported that approximately 14% of HCCs [15 of 106] revealed a pseudocapsule, an enhanced rim in the delayed phase of dynamic MRI, despite it being negative for a histologic fibrous capsule.

Despite some recent studies suggesting that ADC value can predict histopathologic tumour grade, microvascular invasion or early recurrence [11–13], we found no significant correlation between ADC value and tumour grade (Fig. 1). Diffusion-weighted signal intensity and the ADC values particularly depend on selected *b* values and magnetic field strength. In addition, MRI scanner diffusion-weight-based prediction thresholds may not be generalized. Similar to our study, Nasu et al. [17] reported that HCC histopathologic grades did not correlate with ADC values due to the considerable overlap of ADC among the different histopathologic grades.

The pathological severity of liver fibrosis in the nontumorous tissue was evaluated according to the Laennec staging system [18]. Our findings showed a significant difference in the ADC values of mild and moderate fibrosis. Moreover, information about liver parenchyma fibrosis degree could be determined with DWI. Several studies

reported observing a significant correlation [19–21], and the ADC values of mild [4A] parenchyma fibrosis ranged from 1200 to 1400×10^{-3} s/mm^2 [median 1340×10^{-3} s/mm^2], while moderate [4B] fibrosis ranged from 962.5 to 1150×10^{-3} s/mm^2 [median 1065×10^{-3} s/mm^2] (Fig. 2). However, it should be noted that steatosis and iron deposition might affect ADC values.

The limitations of our study include the limited number of patients evaluated, the interpretation of the images by a single radiologist, the lack of long-term follow-up and the retrospective design. Moreover, as this study was conducted at a single institution, multi-centre studies are necessary to validate the findings of this research. Interpretation by a single radiologist could potentially impact the objectivity and reliability of the results, as interpretations by two radiologists may provide more comprehensive and diverse assessments. The study could benefit from mentioning this limitation to acknowledge the potential bias that might arise from relying on a single radiologist's interpretation and to provide a more comprehensive perspective on the findings.

Conclusion

This study showed that ADC values could only be used to distinguish mild cirrhotic livers from moderate cirrhotic livers. Diffusion MRI, a reliable imaging method,
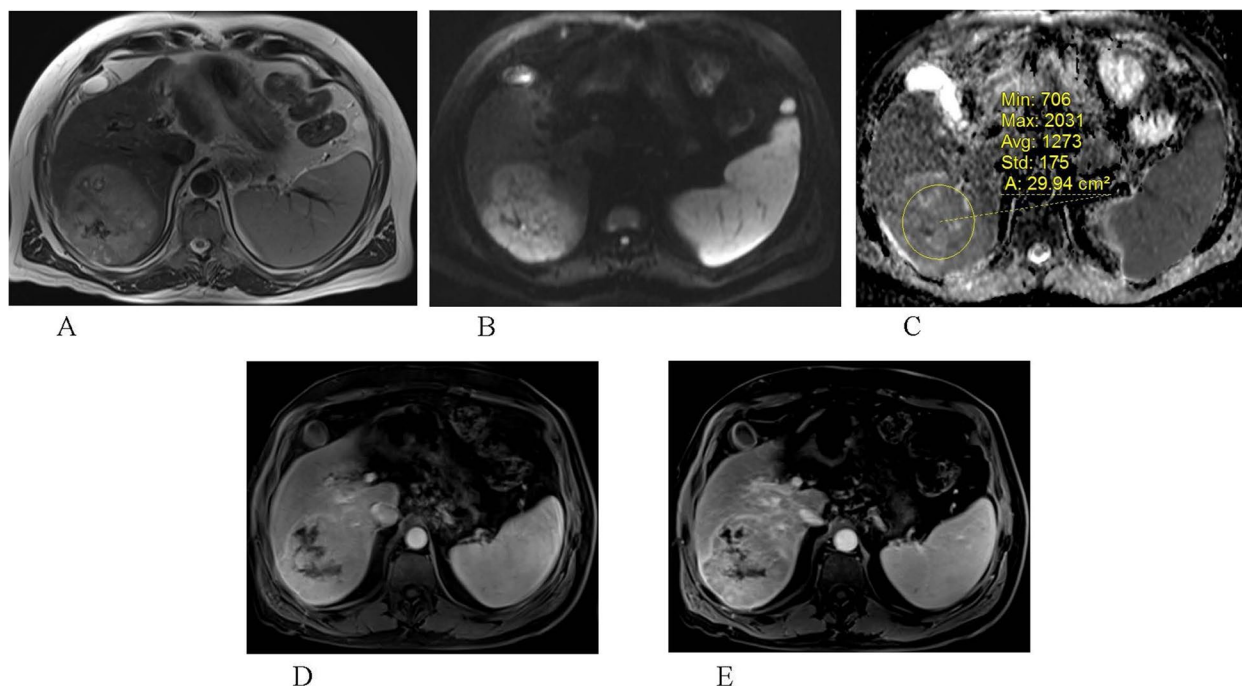

Fig. 1 A 56-year-old male with grade 4 hepatocellular carcinoma on T2-weighted (**A**). **B** Diffusion-weighted images (DWI) of the tumour show diffusion restriction and hyperintense signal with unclear margin. The mean apparent diffusion coefficient (ADC) value is 1273×10^{-3} mm^2/s in the region of interest (**C**). After contrast administration, the lesion has inhomogeneous contrast enhancement in the portal (**D**) and venous (**E**) phases
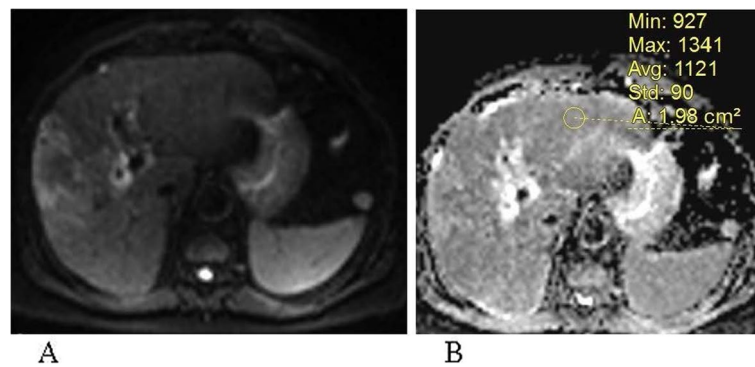
Fig. 2 A 48-year-old female with hepatitis B virus-induced cirrhosis on MRI. Moderate (4B) liver parenchymal fibrosis diagnosed with a pathological specimen. Diffusion weighted image (**A**) is seen. The mean ADC value (**A**) of parenchyma was 1341×10^{-3} mm^2/s

can be used to diagnose liver fibrosis degree without histopathological analysis. Contrast-enhanced MRI plays a crucial role in the diagnosis of HCC. According to our study results, only intralesional fat and tumour size are imaging features prognostic for HCC. MRI is an excellent tool for diagnosing HCC; however, patients' prognoses can be estimated using a combination of imaging and clinical features. This indicates that clinical data and other relevant information should be taken into account when estimating patient outcomes.

The integration of imaging and clinical features can enhance the accuracy and reliability of prognostic assessments, enabling healthcare professionals to make more informed decisions regarding patient management and treatment strategies.

As with any study, it is important to acknowledge the limitations and consider the specific context in which the research was conducted. Further validation and replication of findings across diverse patient populations can strengthen the significance and generalizability of the results.

Abbreviations

ADC	Apparent diffusion coefficient
HCC	Hepatocellular carcinoma
MRI	Magnetic resonance imaging
AASLD	American Association for the Study of Liver Disease
DWI	Diffusion-weighted imaging
ROI	Region of interest
E-S	Edmondson-Steiner
EASL	European Association for the Study of the Liver
Li-RADS	Liver Imaging Reporting and Data System
MIV	Microvascular invasion
PACS	Picture archiving and communication system
AFP	Alpha fetoprotein
NASH	Nonalcoholic steatohepatitis

Acknowledgements
Not applicable.

Authors' contributions
All authors contribute to the whole article including the findings, methodology and investigation. All authors have read and approved the manuscript. AAK and AO introduced the idea of this research reporting, writing and revision of the manuscript. SK and AO: clinical examination of recruited patients.

Availability of data and materials
The datasets used and/or analysed during the current study are available from the corresponding author upon reasonable request.

Declarations

Ethics approval and consent to participate
This study was approved by the Institutional Review Board of Acibadem University with the decision number 2020–23/28.

Consent for publication
Not applicable.

Competing interests
The authors declare that they have no competing interests.

References
1. Kulik L, El-Serag HB (2019) Epidemiology and management of hepatocellular carcinoma. Gastroenterology 156(2):477–491. https://doi.org/10.1053/j.gastro.2018.08.065
2. Hartke J, Johnson M, Ghabril M (2017) The diagnosis and treatment of hepatocellular carcinoma. Semin Diagn Pathol 34(2):153–159. https://doi.org/10.1053/j.semdp.2016.12.011
3. Yang JD, Heimbach JK (2020) New advances in the diagnosis and management of hepatocellular carcinoma. BMJ 371:m3544. https://doi.org/10.1136/bmj.m3544
4. Ronot M, Purcell Y, Vilgrain V (2019) Hepatocellular carcinoma: current imaging modalities for diagnosis and prognosis. Dig Dis Sci 64(4):934–950. https://doi.org/10.1007/s10620-019-05547-0

Altan Kus *et al. Egyptian Liver Journal*   (2023) 13:52

Page 7 of 7

5. Jiang HY, Chen J, Xia CC, Cao LK, Duan T, Song B (2018) Noninvasive imaging of hepatocellular carcinoma: from diagnosis to prognosis. World J Gastroenterol 24(22):2348–2362. https://doi.org/10.3748/wjg.v24.i22.2348

6. Choi JY, Lee JM, Sirlin CB (2014) CT and MR imaging diagnosis and staging of hepatocellular carcinoma: part I. Development, growth, and spread: key pathologic and imaging aspects. Radiology 272(3):635–54. https://doi.org/10.1148/radiol.14132361

7. Choi JY, Lee JM, Sirlin CB (2014) CT and MR imaging diagnosis and staging of hepatocellular carcinoma: part II. Extracellular agents, hepatobiliary agents, and ancillary imaging features. Radiology 273(1):30–50. https://doi.org/10.1148/radiol.14132362

8. Kim SU, Oh HJ, Wanless IR, Lee S, Han KH, Park YN (2012) The Laennec staging system for histological sub-classification of cirrhosis is useful for stratification of prognosis in patients with liver cirrhosis. J Hepatol 57:556–563. https://doi.org/10.1016/j.jhep.2012.04.029

9. Levi Sandri GB, Lai Q, Bosco S, Berloco PB (2014) Liver splenosis mimicking hepatocellular carcinoma in cirrhotic liver. Liver Int 34(1):162. https://doi.org/10.1111/liv.12250

10. Morii K, Nakamura S, Yamamoto T, Okushin H (2014) Steatotic regenerative nodules mimicking hepatocellular carcinoma. Liver Int 34(3):477. https://doi.org/10.1111/liv.12256

11. Cho ES, Choi JY (2015) MRI features of hepatocellular carcinoma related to biologic behavior. Korean J Radiol 16(3):449–64. https://doi.org/10.3348/kjr.2015.16.3.449

12. Chou YC, Lao IH, Hsieh PL, Su YY, Mak CW, Sun DP et al (2019) Gadoxetic acid-enhanced magnetic resonance imaging can predict the pathologic stage of solitary hepatocellular carcinoma. World J Gastroenterol 25(21):2636–2649. https://doi.org/10.3748/wjg.v25.i21.2636

13. Cuccurullo V, Di Stasio GD, Mazzarella G, Cascini GL (2018) Microvascular ınvasion in HCC: the molecular ımaging perspective. Contrast Media Mol Imaging 2018:9487938. https://doi.org/10.1155/2018/9487938

14. Kim KA, Kim MJ, Jeon HM, Kim KS, Choi JS, Ahn SH et al (2012) Prediction of microvascular invasion of hepatocellular carcinoma: usefulness of peritumoral hypointensity seen on gadoxetate disodium-enhanced hepatobiliary phase images. J Magn Reson Imaging 35:629–634. https://doi.org/10.1002/jmri.22876

15. Gouw AS, Balabaud C, Kusano H, Todo S, Ichida T, Kojiro M (2011) Markers for microvascular invasion in hepatocellular carcinoma: where do we stand? Liver Transpl 17(Suppl 2):72–80. https://doi.org/10.1002/lt.22368

16. Ishigami K, Yoshimitsu K, Nishihara Y, Irie H, Asayama Y, Tajima T et al (2009) Hepatocellular carcinoma with a pseudocapsule on gadolinium-enhanced MR images: correlation with histopathologic findings. Radiology 250(2):435–443. https://doi.org/10.1148/radiol.2501071702

17. Nasu K, Kuroki Y, Tsukamoto T, Nakajima H, Mori K, Minami M (2009) Diffusion-weighted imaging of surgically resected hepatocellular carcinoma: imaging characteristics and relationship among signal intensity, apparent diffusion coefficient, and histopathologic grade. AJR Am J Roentgenol 193(2):438–444. https://doi.org/10.2214/AJR.08.1424

18. Kim MY, Cho MY, Baik SK, Park HJ, Jeon HK, Im CK et al (2011) Histological subclassification of cirrhosis using the Laennec fibrosis scoring system correlates with clinical stage and grade of portal hypertension. J Hepatol 55:1004–1009. https://doi.org/10.1016/j.jhep.2011.02.012.54

19. Sandrasegaran K, Akisik FM, Lin C et al (2009) Value of diffusion-weighted MRI for assessing liver fibrosis and cirrhosis. Am J Roentgenol 193:1556–1560. https://doi.org/10.2214/AJR.09.2436

20. Lurie Y, Webb M, Cytter-Kuint R, Shteingart S, Lederkremer GZ (2015) Noninvasive diagnosis of liver fibrosis and cirrhosis. World J Gastroenterol 21(41):11567–11583. https://doi.org/10.3748/wjg.v21.i41.11567

21. Verloh N, Utpatel K, Haimerl M, Zeman F, Fellner C, Fichtner-Feigl S et al (2015) Liver fibrosis and Gd-EOB-DTPA-enhanced MRI: a histopathologic correlation. Sci Rep 5:15408. https://doi.org/10.1038/srep15408

Publisher's Note